

27389

Abstract |

Establishing a global algorithm for water quality mapping from multi-dates images



mohd
- Zubir

- Khiruddin

H. S. Lim, M. Z. MatJafri, K. Abdullah and M. N. A. Bakar
School of Physics
Universiti Sains Malaysia,
11800 Penang

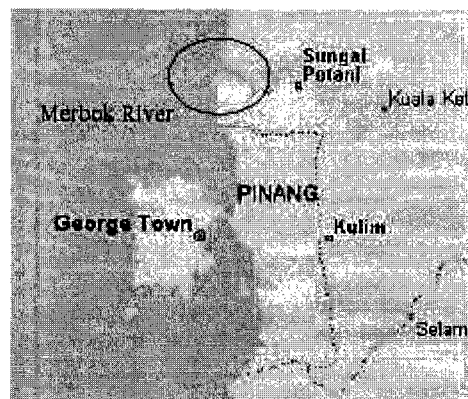
Presented at the MAP ASIA
2003, 13-15 Oct. 2003,
K-L.

Introduction

Water quality assessment of ocean and inland waters using satellite data has been carried out since the first satellite Landsat-MSS has been operational (Thiemann and Kaufmann, 2000). Many researchers used satellite investigations [Allee, et al., (1999), Forster, et al., (1993) and Ritchie, et al., (1990)]. However, in this study we remote sensing. A digital camera was used as a sensor to capture the images at altitude of 8000 feet. The main present study is to update our proposed algorithm for mapping total suspended solids in marine environment camera images from previous study (MatJafri, et al., 2002). We also attempted to develop a simple correction to airborne images acquired from different dates, locations, and different flying altitudes. Data from seven images combined in the present analysis. This study also proposed a cheaper and economical alternative to overcome obtaining cloud-free scenes in the Equatorial region.

Study Area

In this study, a Kodak DC290 digital camera was used as a sensor and a Cessna 172Q aircraft was used to capture images of the study areas. The study areas were the Prai, Muda, and Merbok river estuaries, located with 22' N to 5o 24'N and longitudes 100o 21'E to 100o 23'E; 5o 34' N to 5o 36'N and longitudes 100o 19'E to 100o 21'E; 5o 41'N and longitudes 100o 20'E to 100o 24'E, respectively. The images were captured from the altitude of 8,000ft on 9 March 2001 and 8,000ft on 20 January 2002 for Prai River estuary, 8,000ft on 9 March 2002 for Merbok River estuary, and also 8,000 ft on 5 May 2002, 25 October 2002 and 22 March 2003 for Merbok River estuary. They are shown in Figure 1. Water samples were collected from a small boat within the areas covered by the scenes with the airborne image acquisition and later analyzed in the laboratory.



(Source: Microsoft Corp., 2001.)

Figure 1. Study area

Optical model of water

A physical model relating radiance from the water column and the concentrations of the water quality constituents is the most effective way of analyzing remotely sensed data for water quality studies. Reflectance is particularly useful for water quality studies because it is particularly sensitive to the inherent optical properties: the absorption coefficient and the backscattering coefficient. The irradiance reflectance from the water surface, $R(l)$, is given by Kirk (1984) as

$$R(\lambda) = 0.33b(\lambda)/a(\lambda) \quad (1)$$

where λ = the spectral wavelength
 b = the backscattering coefficient
 a = the absorption coefficient

The inherent optical properties are determined by the contents of the water. The contributions of the individual the overall properties are strictly additive (Gallegos and Correl, 1990). For a case involving two water quality chlorophyll, C, and suspended sediment, P, the simultaneous equations for the two channels given by Gallie and can be expressed as

$$R(\lambda_1) = R_1 = 0.33 \frac{(0.5b_{bw}(\lambda_1) + b_{bc}^*(\lambda_1)C + b_{bp}^*(\lambda_1)P)}{(a_w(\lambda_1) + a_c^*(\lambda_1)C + a_p^*(\lambda_1)P)} \quad (2a)$$

$$R(\lambda_2) = R_2 = 0.33 \frac{(0.5b_{bw}(\lambda_2) + b_{bc}^*(\lambda_2)C + b_{bp}^*(\lambda_2)P)}{(a_w(\lambda_2) + a_c^*(\lambda_2)C + a_p^*(\lambda_2)P)} \quad (2b)$$

where

$b_{bw}(i)$ = backscattering coefficient of water
 b_{bc}^* = specific backscattering coefficients of chlorophyll
 b_{bp}^* = specific backscattering coefficients of sediment
 $a_w(i)$ = absorption coefficient of water
 a_c^* = specific absorption coefficients of chlorophyll
 a_p^* = specific absorption coefficients of sediment
 C = chlorophyll
 P = suspended sediment

Regression Algorithm

TSS concentration can be obtained by solving the two simultaneous equations to get the series of terms R_1 and R_2 as

$$P = a_0 + a_1R_1 + a_2R_2 + a_3R_1R_2 + a_4R_1^2 + a_5R_2^2 + a_6R_1^2R_2 + a_7R_1^2R_2^2 + a_8R_1^2R_2^2 + \dots \quad (3)$$

where a_j , $j = 0, 1, 2, \dots$ are the coefficient for equation (3) that can be solved empirically using multiple regression equation can also be extended to the three-band method given as

$$P = e_0 + e_1R_1 + e_2R_2 + e_3R_3 + e_4R_1R_2 + e_5R_1R_3 + e_6R_2R_3 + e_7R_1^2 + e_8R_2^2 + e_9R_3^2 \quad (4)$$

where the coefficient e_j , $j = 0, 1, 2, \dots$ can also be solve empirically.

Data Analysis And Result

Seven sets of the colour images were selected for calibration analysis. Figure 2 shows the images that were used

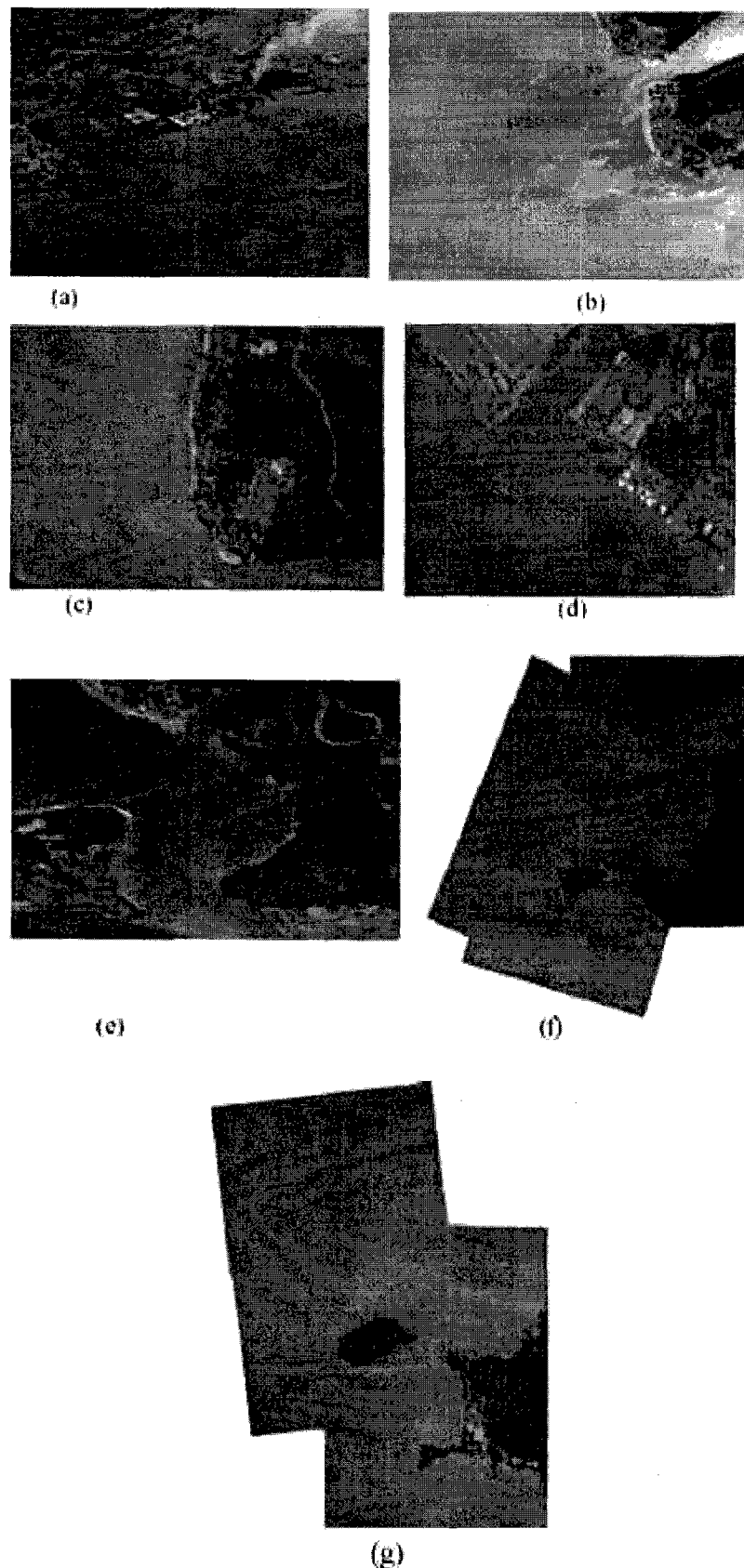


Figure 2. Images of the study areas: (a) the oblique image of the Prai River estuary captured on 28 October 2001 from altitude of 8,000ft, (b) the oblique image of the Muda River estuary captured on 20 January 2002 from altitude of 8,000ft, (c) the vertical image of the Prai River estuary captured on 9 March 2002 from altitude of 8,000ft, (d) the vertical image of the Muda River estuary captured on 9 March 2002 from altitude of 8,000ft, (e) the oblique image of the Merbok River estuary captured on 5 May 2002 from altitude of 8,000ft, (f) the vertical image of the Merbok River estuary captured on 5 May 2002 from altitude of 8,000ft, (g) the vertical image of the Merbok River estuary captured on 5 May 2002 from altitude of 8,000ft.

River estuary captured on 26 October 2002 from altitude of 8,000ft and (g) the vertical image of the Merbok River estuary captured 2003 from altitude of 8,000ft.

The colour images were separated into three bands, namely, red, green and blue bands for multispectral analysis. Figure 2(a) was taken at an altitude of 3,000ft, while the rest were taken from altitude of 8,000ft. The image in Figure 2(b) and Figure 2(e) were taken obliquely. The view angle correction was first performed to the oblique image for the angular dependence of image brightness. In this study, a contour map of the image brightness was plotted and the angle effect was removed based on the map. Then, the multi-date data were corrected to remove the difference effects between scenes using radiometric normalization technique. The vertical image of Figure 5(c) was selected as the reference image and the average brightness of the chosen target; in this case, grass vegetation was noted. The reflectance of these targets did not change with time. This assumption is in accordance with the methods proposed by (1990). The average brightness values of grass in other images were then recorded. The difference from the reference was used to correct for each scene. All the brightness values of the other five images of Figure 5 (a), (b), (d), (e) and (f) were adjusted using this normalization technique. This normalization technique forced the images to have the same atmospheric conditions and the effects due to different camera altitudes have also been removed. The corrected images were then regressed with the sea-truth data to obtain all the coefficients of equation (4) in the proposed multi-date, multi-altitude analysis. Image rectification was performed using second order polynomial transformation equation.

The DN values corresponding to the water sample locations were extracted from all the images. The relationship between TSS and DN of the data set is shown in Figure 3. The coefficients values are listed in Table 1. Figure 4 shows the algorithm produced high correlation coefficient (R) and low root-mean-square (RMS).

The TSS maps were generated using the proposed calibrated algorithm. The generated maps were then filtered using a 3x3 pixels average for removing random noise. Finally, the generated TSS maps were colour-coded for visual interpretation in Figure 5. This indicates the reliability of the calibrated proposed algorithm for TSS mapping using digital camera.

Table 1. Correlation coefficients of equation (2)

Coefficients	a0	a1	a2	a3	a4	a5	a6	a7	a8	a9
Values	43.794	-2.021	-9.964	10.710	0.121	-7.278x10 ⁻²	0.279	-1.640x10 ⁻²	-0.141	-0.15

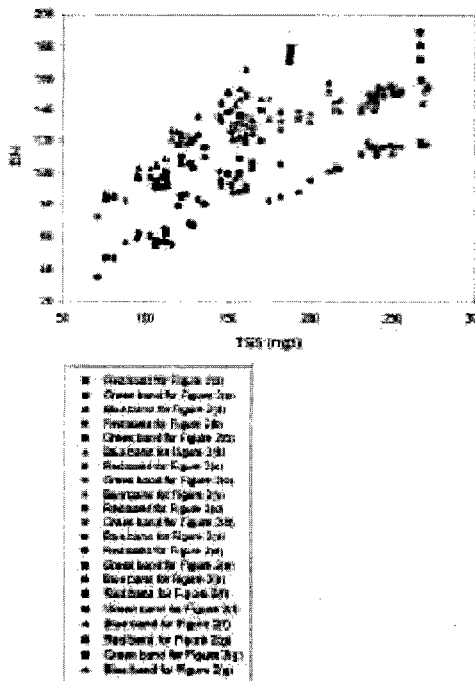


Figure. 3 TSS concentration versus digital number (DN).

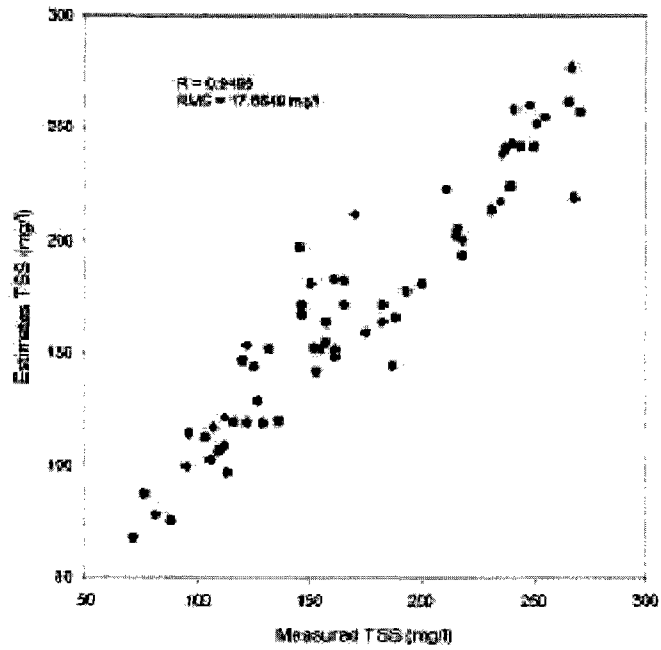
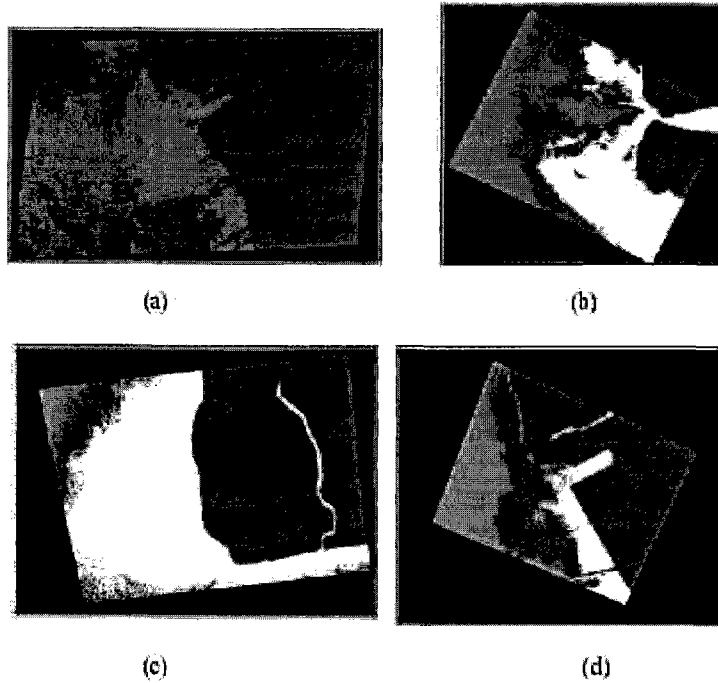


Figure 4. Measured versus estimated TSS concentration



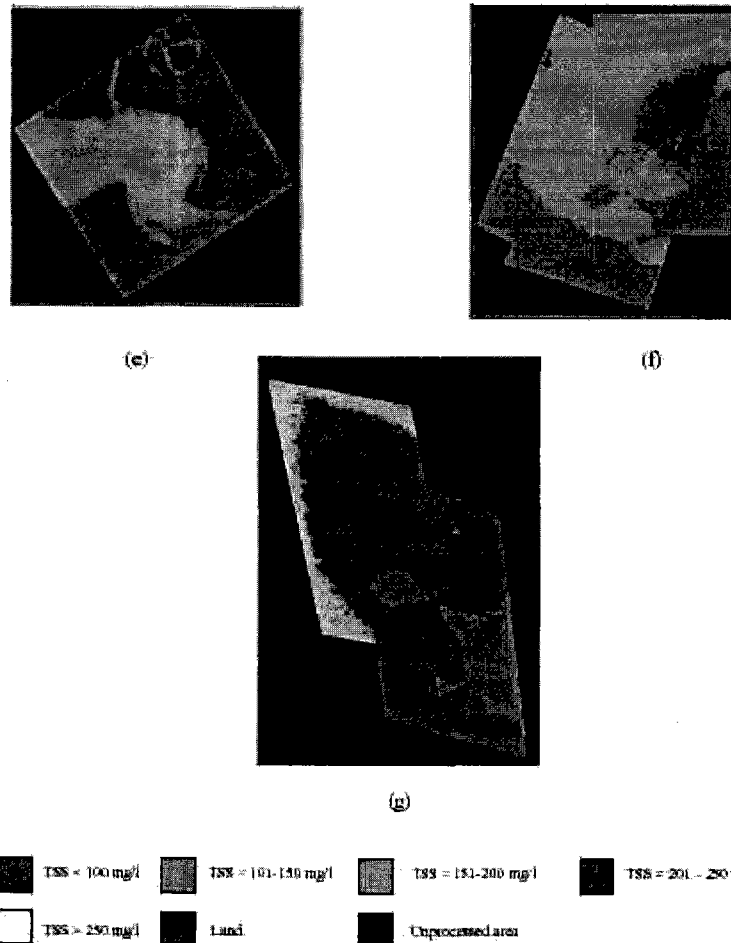


Figure 5. TSS map for the study area estimated using the proposed algorithm. Colour code:

Verification analysis

For the verification analysis, sea truth data were divided into two groups, half of the numbers of water sample selected for algorithm calibration and the another half of the numbers of water samples were radom selected analysis. The calibrated algorithm was produced high accuracy with R value of 0.9685 and RSM value of 13 verification analysis. Figure 6 shows the relationship of the measured TSS versus estimated TSS concentratio calibration analysis. Figure 7 shows the relationship of the measured TSS versus estimated TSS concentration analysis.

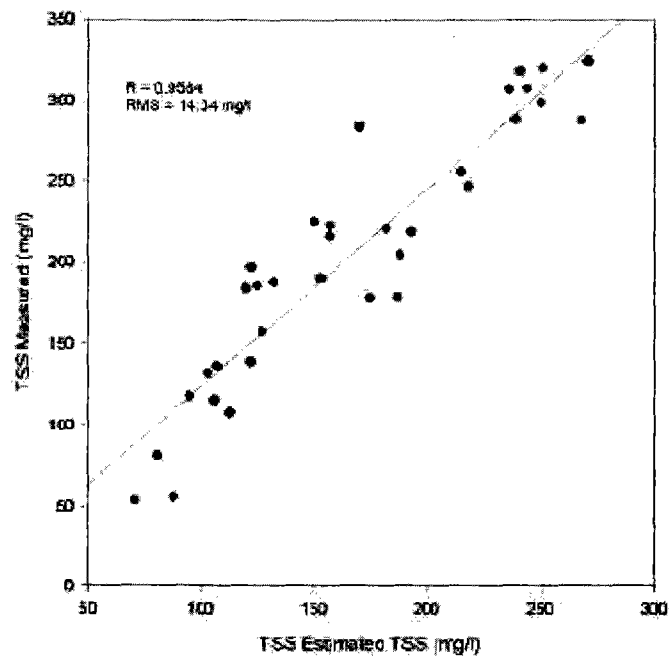


Figure 6. Measured TSS versus estimated TSS concentration for algorithm calibration analysis

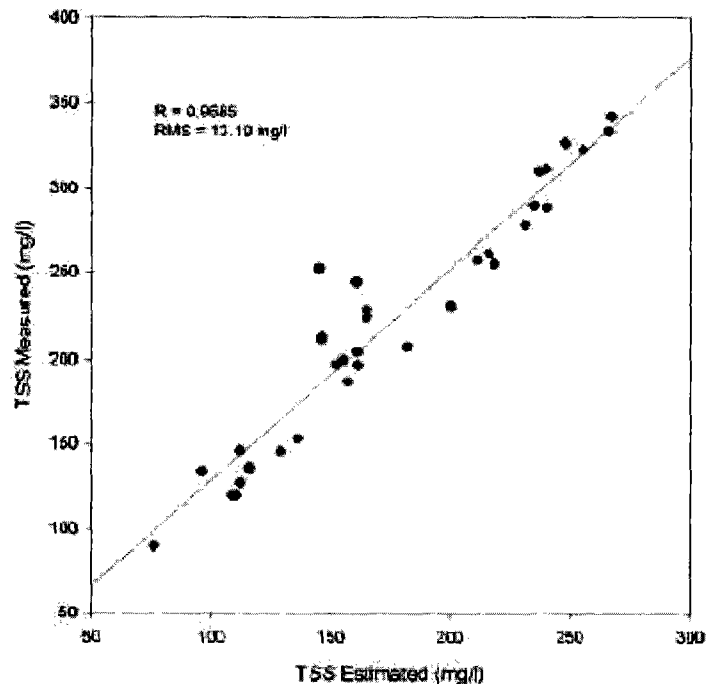


Figure 7. Measured TSS versus estimated TSS concentration for verification analysis Conclusion

This study gives a cheaper way to overcome the problem of difficulty of obtaining cloudfree scenes at the Eqi Traditional water quality monitoring method based on water sample collection is time consuming and requires a cost. It is good for determined the water pollution for real time. The proposed algorithm is considered superior algorithms based on the values of the correlation coefficient, $R=0.97$ and root-mean-square error, $RMS=15\text{mg/l}$. that the TSS maps can be generated using digital camera imagery with the proposed algorithm.

Acknowledgement

This project was carried out using the Malaysian Government IRPA grant no. 08-02-05- 6011 and USM sr FPP2001/130. We would like to thank the technical staff and research officers who participated in this proje extended to USM for support and encouragement.

References

- Allee, R.J., and Johnson, J.E., (1999). Use of satellite imagery to estimate surface chlorophyll-a and Secchi Bull Shoals, Arkansas, USA.
- International Journal of Remote Sensing, 20, 1057-1072.
- Forster, B.C., Xingwei, I.S., and Baide, X., 1993, Remote sensing of water quality parameters using International Journal of Remote Sensing, 14, 2759-2771.
- Gallegos, C.L., and Correl, D.L., (1990). Modeling spectral diffuse attenuation, absorption and scattering in a turbid estuary. Limnology and Oceanography, 35, 1486-1502.
- Gallie, E.A., and Murtha, P.A., (1992). Specific absorption and backscattering spectra for suspended chlorophyll-a in Chilko Lake, British Columbia.
- Remote Sensing of Environment, 39, 103-118.
- Kirk, J. T. O. (1984). Dependence of relationship between inherent and apparent optical properties of water. Limnology and Oceanography, 29, 350-356.
- Lopez Garcia, M.J., 1990, A multi-temporal study of chlorophyll-a concentration in the Albufera lagoon, Spain, Using Thematic Mapper data.
- International Journal of Remote Sensing, 11, 301-311.
- Microsoft Corp., Map of Kedah, Malaysia. (2001). [online]. http://worldtwitch.virtualave.net/kedah_map.htm
- M. Z. MatJafri, K. Abdullah, H. S. Lim, M.N. AbuBakar, Z.B. Din, and S. Marshall, (2002). Algorithm For Total Suspended Solids Mapping Using Digital Camera Images. Proceeding in SPIE's Third International Asia-Pacific Environmental Sensing Symposium - Remote Sensing Of The Atmosphere, Ocean, Environment, and Space: Ocean Remote Sensing Applications, 23 – 27 October 2002, HangZhou, China.
- Ritchie, C.J., Cooper, C.M., and Schiebe, F.R., 1990, The relationship of MSS and TM digital data with sediment, chlorophyll and temperature in Moon Lake, Mississippi. Remote Sensing of environment, 33, 13-23.
- Thiemann, S. and Kaufmann, H. (2000). Determination of chlorophyll content and trophic state of a lake using a spectrometer and IRS-1C satellite data in the Mecklenburg Lake District, Germany. Remote Sensing of Environment, 74, 227-235.